

# Tests of three-flavor mixing in long-baseline neutrino oscillation experiments

G. L. Fogli

*Dipartimento di Fisica dell'Università and Sezione INFN di Bari, I-70126 Bari, Italy*

E. Lisi

*Institute for Advanced Study, Princeton, New Jersey 08540*

*and Dipartimento di Fisica dell'Università and Sezione INFN di Bari, I-70126 Bari, Italy*

(Received 26 April 1996)

We compare the effectiveness of various tests of three-flavor mixing in future long-baseline neutrino oscillation experiments. We analyze a representative case of mixing in a simplified three-flavor scheme, whose relevant parameters are one neutrino mass-square difference  $m^2$  and two mixing angles  $\psi$  and  $\phi$ . We show that an unambiguous determination of  $\psi$  and  $\phi$  requires flavor-appearance tests in accelerator experiments, as well as supplementary information from reactor experiments. [S0556-2821(96)03617-X]

PACS number(s): 14.60.Pq, 12.15.Ff, 14.60.Lm

## I. INTRODUCTION

The next generation of proposed accelerator neutrino oscillation experiments will be characterized by unprecedented source-detector distances: 730 km for the Fermilab to Soudan experiment (MINOS) [1,2], 250 km for the KEK-PS to SuperKamiokande experiment [3], 68 km for the Brookhaven National Laboratory experiment E889 [4], and 732 km for the CERN to Gran Sasso experiment, with the Imaging of Cosmic and Rare Underground Signals (ICARUS) [5], ring-imaging Cherenkov counter (RICH) [6], or NOE [7] as candidate detectors. Two reactor experiments under construction, Chooz [8] and San Onofre [9], also have a much longer baseline (1 km) than previous experiments of their class.

These long-baseline experiments are sensitive, in the favorable case of large  $\nu$  mixing, to neutrino square mass differences as low as  $10^{-3}$  eV<sup>2</sup>. Moreover, they probe several flavor-oscillation channels. Oscillation signals in two or more independent channels could indicate flavor mixing among three generations ( $3\nu$  mixing).

In this work, we analyze the effectiveness of long-baseline experiments in detecting  $3\nu$  mixing signals. In Sec. II we describe a representative case of mixing in a simple  $3\nu$  scheme. (This scheme is extensively discussed in [10,11], to which we refer the reader for further details.) In Secs. III and IV we focus on oscillation searches at ICARUS and MINOS, respectively. We also comment briefly upon searches at BNL E889, SuperKamiokande, RICH, and NOE. We show that flavor-appearance tests are essential to constrain multiple interpretations of the signals. In Sec. V we show how reactor experiments may eliminate an ambiguity in the determination of the mixing angles. We summarize our work in Sec. VI.

## II. THREE-FLAVOR MIXING: A TEST CASE

In a three-generation approach, the  $\nu$  states with definite flavor ( $\nu_\alpha = \nu_e, \nu_\mu, \nu_\tau$ ) are a superposition of  $\nu$  states with definite mass ( $\nu_i = \nu_1, \nu_2, \nu_3$ ):  $\nu_\alpha = U_{\alpha i} \nu_i$ ,  $U$  being a unitary matrix. We assume [10] that the two independent neutrino

square mass differences,  $\delta m^2 = m_2^2 - m_1^2$  and  $m^2 = m_3^2 - m_1^2$ , are widely separated:

$$\delta m^2 \leq 10^{-4} \text{ eV}^2, \quad m^2 \geq 10^{-3} \text{ eV}^2 \rightarrow \delta m^2 \ll m^2. \quad (1)$$

Accelerator and reactor neutrino oscillations are then simply described in terms of  $(m^2, U_{e3}, U_{\mu3}, U_{\tau3})$  or, equivalently, in terms of  $(m^2, \psi, \phi)$ , along with the parametrization ( $s_\phi = \sin\phi$ , etc.)

$$U_{e3}^2 = s_\phi^2, \quad U_{\mu3}^2 = c_\phi^2 s_\psi^2, \quad U_{\tau3}^2 = c_\phi^2 c_\psi^2. \quad (2)$$

The oscillation probabilities are given by [10]

$$P(\nu_\alpha \rightarrow \nu_\beta) = \begin{cases} 4U_{\alpha 3}^2 U_{\beta 3}^2 S & \text{if } \alpha \neq \beta, \\ 1 - 4U_{\alpha 3}^2 (1 - U_{\alpha 3}^2) S & \text{if } \alpha = \beta, \end{cases} \quad (3)$$

where  $S = \sin^2(1.27 m^2 L / E_\nu)$ , with  $m^2$ ,  $L$ , and  $E_\nu$  measured in eV<sup>2</sup>, km, and GeV, respectively. In this scheme,  $\nu$  and  $\bar{\nu}$  oscillations in vacuum are indistinguishable.

It has been shown [10] that a useful representation of the parameter space  $(m^2, \psi, \phi)$  is obtained through  $(\tan^2\psi, \tan^2\phi)$  sections at fixed values of  $m^2$ . A generic point in the  $(\tan^2\psi, \tan^2\phi)$  plane represents the state  $\nu_3$ ; the lower left and right corners and the upper side represent, asymptotically,  $\nu_\tau$ ,  $\nu_\mu$ , and  $\nu_e$ , respectively.

For definiteness, we choose a representative  $3\nu$  case:

$$m^2 = 2.5 \times 10^{-2} \text{ eV}^2,$$

$$\nu_3 = \sqrt{0.75} \nu_\tau + \sqrt{0.20} \nu_\mu + \sqrt{0.05} \nu_e, \quad (4)$$

corresponding to  $\psi = 27.3^\circ$  and  $\phi = 12.9^\circ$ . In Fig. 1, this test case is marked by a black circle ( $\bullet$ ) in the  $(\tan^2\psi, \tan^2\phi)$  plane at  $m^2 = 2.5 \times 10^{-2}$  eV<sup>2</sup>.

The case in Eq. (4) has the following properties (see also [10]): (1) it is allowed by the available reactor data, as shown in Fig. 1; (2) it is in the sensitivity region of long-baseline experiments; (3) it is outside the sensitivity region of the running oscillation experiments, CHORUS, NOMAD, KARMEN, and the Liquid Scintillator Neutrino Detector (LSND) (see [10] and references therein); (4) it is compatible

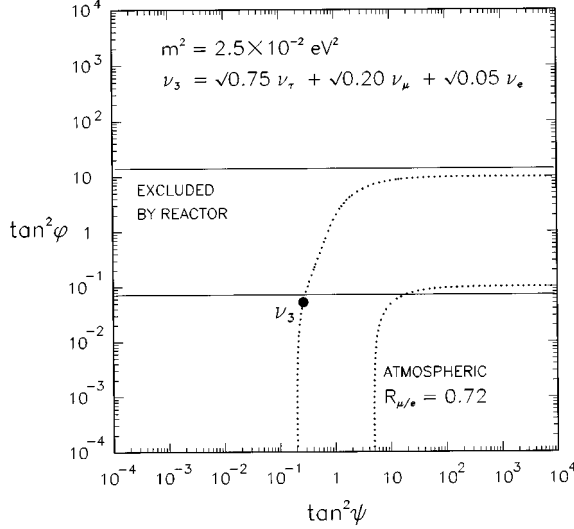


FIG. 1. The representative three-flavor mixing case (•) in the  $(\tan^2\psi, \tan^2\phi)$  plane. The horizontal band is excluded by present reactor  $\nu$  data. The  $\Gamma$ -shaped region is consistent with the indications of the atmospheric neutrino flavor anomaly ( $R_{\mu/e} = 0.72$  along the dotted lines). See also Ref. [10].

with the indications of an anomalous  $\mu/e$  flavor ratio in the atmospheric  $\nu$  flux, and in particular with a value  $R_{\mu/e} = (\mu/e)_{\text{data}} / (\mu/e)_{\text{theory}} \approx 0.72$ , as shown in Fig. 1; and (5) the matrix elements  $U_{\alpha 3}$  are hierarchically ordered. We will emphasize the results that remain valid in more general situations.

The adopted value of  $m^2$  is sufficiently high to allow in Eq. (3), for our purposes, the ‘‘averaged oscillation’’ approximation,  $\langle S \rangle \approx 1/2$ . In a more refined approach,  $S$  has to be computed using the  $E_\nu/L$  spectrum. Spectral analyses are also necessary to infer the value of  $m^2$ . A discussion of such tests is beyond the scope of this work.

Our strategy is the following. For any experiment we define one or more observables,  $Q_i$ , that differ from zero in the presence of oscillations. We assume a conservative, plausible estimate of  $\pm 20\%$  for the total experimental errors,  $\delta Q_i$ , of the measured signals  $Q_i$ . The actual values of the errors are not decisive for our considerations. The  $\delta Q_i$ ’s will be precisely estimated when the experiments will perform real measurements. In synthesis,

$$Q_i = 0 \rightarrow \text{no oscillation,}$$

$$Q_i \neq 0 \rightarrow \text{oscillation } (\delta Q_i / Q_i \approx \pm 20\%). \quad (5)$$

We then compute the  $Q_i$ ’s in the representative  $3\nu$  test case [Eq. (4)] using the averaged oscillation probabilities,  $P_{\alpha\beta} = \langle P(\nu_\alpha \rightarrow \nu_\beta) \rangle$  [Eq. (3)]. Our goal is to study how the starting test values of the mixing angles may be inferred from measurements of the observables  $Q_i$ .

### III. OSCILLATION TESTS AT ICARUS

The ICARUS detector can identify  $e$  events downstream from a  $\nu_\mu$  beam, thus probing  $\nu_\mu \rightarrow \nu_e$  appearance. There are good prospects for direct  $\tau$  identification. So we also assume

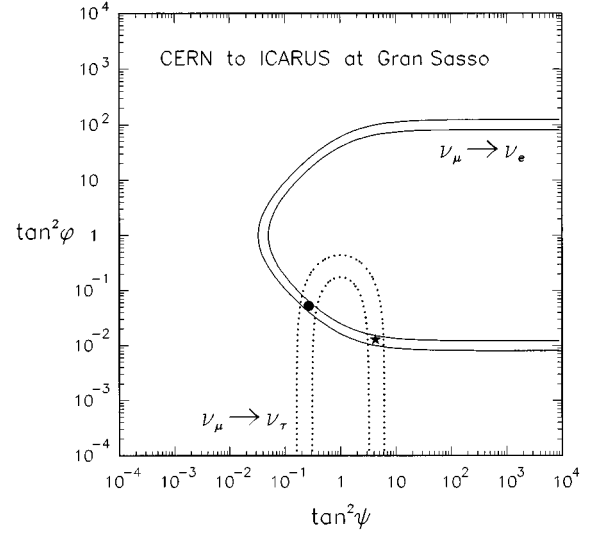


FIG. 2. Allowed bands corresponding to  $\nu_\mu \rightarrow \nu_e$  and  $\nu_\mu \rightarrow \nu_\tau$  appearance searches at the ICARUS experiment, in the test case (•) of Fig. 1. The two bands also intersect at a second point (★), giving rise to a twofold ambiguity in the determination of the mixing angles  $\psi$  and  $\phi$ .

that  $\nu_\mu \rightarrow \nu_\tau$  appearance searches can be performed with the ICARUS detector.

Two observables can be defined in terms of the number of events  $N_{e,\mu,\tau}$  at the detector:

$$Q_{\mu e} \equiv \frac{N_e(\text{observed})}{N_\mu(\text{expected})} = P_{\mu e}, \quad (6)$$

$$Q_{\mu\tau} \equiv \frac{N_\tau(\text{observed})}{N_\mu(\text{expected})} = P_{\mu\tau}. \quad (7)$$

In the  $3\nu$  test case [Eq. (4)], the above observables take the values  $Q_{\mu e} = 0.02(1 \pm 0.2)$  and  $Q_{\mu\tau} = 0.30(1 \pm 0.2)$ .

In Fig. 2 we show the corresponding curves of iso- $Q_{\mu e}$  and iso- $Q_{\mu\tau}$ . The width of the bands is proportional to  $\delta Q_i$ . The bands intersect at two points. One represents, of course, the ‘‘true’’ test case (•). The second point (★) represents a ‘‘false’’ combination of mixing angles. In other words, the determination of  $(\psi, \phi)$  through the values  $(Q_{\mu e}, Q_{\mu\tau})$  is subject to a twofold ambiguity.

The appearance of a second  $3\nu$  solution is not limited to the test case, and cannot be avoided by reducing the errors  $\delta Q_i$ . In fact, the twofold solution arises essentially from the quadratic mixing terms in Eq. (3).

### IV. OSCILLATION TESTS AT MINOS

The MINOS detector can identify  $\mu$  tracks downstream from a  $\nu_\mu$  beam. It is also expected to identify electrons and thus to be as sensitive to  $Q_{\mu e}$  as the ICARUS detector. First we describe two oscillation search methods that use only  $\mu$  identification, the  $T$  test and the far-near test [1]. Then we discuss the  $e$  appearance observable  $Q_{\mu e}$ .

The  $T$  and far-near tests exploit the unoscillated measurements at a second, smaller detector to be placed near the  $\nu$ -beam source. One separates the events with ‘‘one muon

track'' ( $1\mu$ ) and with ''no muon track'' ( $0\mu$ ).

At the near detector, the number of events  $n_{1\mu}$  and  $n_{0\mu}$  are proportional to the  $\nu_\mu$  charged (CC) and neutral current (NC)  $E_\nu$ -averaged cross sections,  $\sigma_C$  and  $\sigma_N$ :

$$n_{1\mu} \propto \sigma_C, \quad n_{0\mu} \propto \sigma_N. \quad (8)$$

At the far detector one also has to include the interactions of  $\nu_e$ 's and  $\nu_\tau$ 's. Downstream,  $1\mu$  events are produced by (1)  $\nu_\mu$  CC interactions, and (2)  $\nu_\tau$  CC interactions followed by  $\tau \rightarrow \mu$  decay. The  $0\mu$  events are produced by (1)  $\nu_\mu$  NC interactions, (2)  $\nu_e$  CC or NC interactions, (3)  $\nu_\tau$  NC interactions, and (4)  $\nu_\tau$  CC interactions followed by  $\tau \rightarrow x$  decay,  $x \neq \mu$ . Thus the number of events  $N_{1\mu}$  and  $N_{0\mu}$  in the far detector are

$$N_{1\mu} \propto P_{\mu\mu} \sigma_C + P_{\mu\tau} \eta \sigma_C B, \quad (9a)$$

$$N_{0\mu} \propto P_{\mu\mu} \sigma_N + P_{\mu e} (\sigma_N + \sigma_C) + P_{\mu\tau} [\sigma_N + \eta \sigma_C (1 - B)], \quad (9b)$$

where  $B=0.18$  is the branching ratio ( $\tau \rightarrow \mu$ )/( $\tau \rightarrow$ all), and the factor  $\eta \approx 0.31$  [1] accounts for the average reduction of the  $\nu_\tau$  CC cross section due to the  $\tau$  mass.

Given Eqs. (8) and (9), one introduces [1] two ratios,  $t$  and  $T$ , at the near and far detector, respectively:

$$t \equiv \frac{n_{1\mu}}{n_{1\mu} + n_{0\mu}} = \frac{\sigma_C}{\sigma_C + \sigma_N}, \quad (10)$$

$$T \equiv \frac{N_{1\mu}}{N_{1\mu} + N_{0\mu}} = \frac{t(P_{\mu\mu} + \eta B P_{\mu\tau})}{1 - t P_{\mu\tau} (1 - \eta)}. \quad (11)$$

In deriving the right-hand side of Eq. (11) we have used the unitarity property  $P_{\mu e} + P_{\mu\mu} + P_{\mu\tau} = 1$  and the definition of  $t$  in Eq. (10). At MINOS energies it is  $t \approx 0.72$  [1].

In the  $T$  test,  $T \neq t$  signals neutrino oscillations. A useful observable can be defined as

$$Q_T \equiv 1 - \frac{T}{t} = 1 - \frac{P_{\mu\mu} + \eta B P_{\mu\tau}}{1 - t P_{\mu\tau} (1 - \eta)}. \quad (12)$$

In the far-near test, one counts only  $1\mu$  events at the two detector distances,  $L_{\text{far}}$  and  $L_{\text{near}}$ . Neutrino oscillations are signaled by a nonzero value of the quantity

$$Q_{f/n} \equiv 1 - \frac{N_{1\mu} L_{\text{far}}^2}{n_{1\mu} L_{\text{near}}^2} = 1 - P_{\mu\mu} - P_{\mu\tau} \eta B. \quad (13)$$

In the  $3\nu$  test case,  $Q_T = 0.18(1 \pm 0.2)$  and  $Q_{f/n} = 0.30(1 \pm 0.2)$ . The corresponding iso-signal bands are shown in Fig. 3. These  $\Gamma$ -shaped bands largely superpose in the lower part, producing multiple ''false'' mixing cases ( $\circ \dots \circ$ ) that have, within errors, the same values of  $Q_T$  and  $Q_{f/n}$  as the ''true'' test case ( $\bullet$ ). The multiple solutions (except the highest in  $\phi$ ) are allowed by present reactor data, and are consistent with the atmospheric  $\nu$  anomaly (cf. Figs. 1 and 3). The larger the errors ( $\delta Q_i$ ), the more ambiguous is the  $3\nu$  interpretation of the combined  $Q_T$  and  $Q_{f/n}$  signals.

The  $T$  and far-near tests are not very effective in discriminating among  $3\nu$  cases, since a large fraction of their signal is induced by a disappearance probability,  $P_{\mu\mu}$  [Eqs. (12)

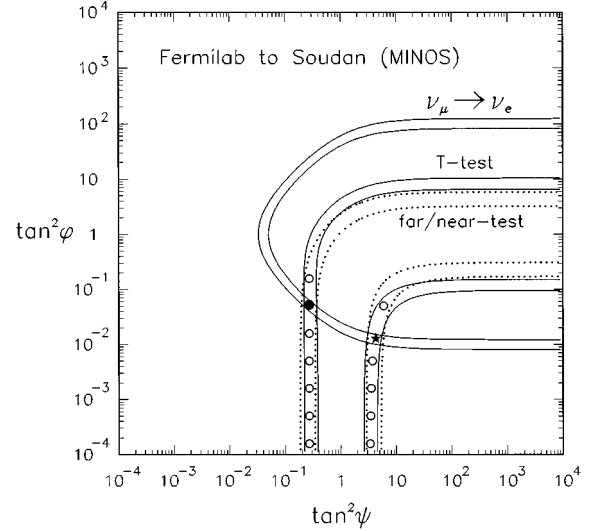


FIG. 3. Allowed bands corresponding to three oscillation tests at the MINOS experiments:  $T$  test, far-near test, and  $\nu_\mu \rightarrow \nu_e$  appearance search. The combination of the  $T$  and far-near tests allows multiple solutions ( $\circ \dots \circ$ ). Adding the  $\nu_\mu \rightarrow \nu_e$  test, only two solutions remain ( $\bullet$  and  $\star$ ) as in Fig. 2.

and (13)]. If limited to  $Q_T$  and  $Q_{f/n}$ , the  $3\nu$ -mixing searches at MINOS may not be much more constraining than a pure  $\mu$ -disappearance experiment as BNL E889 [4] (that, incidentally, is not proceeding [2]).

Therefore it is very important that the MINOS detector probes  $e$  appearance directly. As shown in Fig. 3, the addition of the  $Q_{\mu e}$  test [Eq. (6)] reduces the multiple solutions ( $\circ \dots \circ$ ) to the same two cases ( $\bullet$  and  $\star$ ) as in ICARUS (Fig. 2). The comparison of Figs. 2 and 3 shows that, unfortunately, the ambiguity is not solved by combining the MINOS and ICARUS tests.

If direct  $\tau$  identification were possible at MINOS ( $\nu_\mu \rightarrow \nu_\tau$  appearance), the oscillation searches would be corroborated, since the two solutions ( $\bullet$  and  $\star$ ) would sit at the intersection of four bands in the  $(\tan^2 \psi, \tan^2 \phi)$  plane—an overconstrained situation. However, the  $3\nu$ -mixing ambiguity would still remain unsolved.

The addition of atmospheric  $\nu$  data in the usual format of  $\mu/e$  flavor ratio is not particularly helpful, being very similar to the  $T$  test (cf. Figs. 1 and 3). Flavor-separated data [12] could be more effective in  $3\nu$  mixing cases.

The two possible  $\nu_\mu \rightarrow \nu_\mu$  and  $\nu_\mu \rightarrow \nu_e$  oscillation tests at the planned SuperKamiokande experiment [3] are similar to the MINOS tests. However, the uncertainties [3] are expected to be larger, and the  $3\nu$ -mixing discrimination power should be poorer.

As in MINOS, the RICH [6] and NOE [7] detectors can distinguish  $1\mu$  and  $0\mu$  events and perform a  $1\mu/(1\mu+0\mu)$  test. In absence of a near-detector at CERN, the normalization of their  $\nu$ -rates has to rely upon simulations.

## V. OSCILLATION TEST AT REACTORS

In reactor experiments, a single neutrino oscillation search is performed, namely, the  $\nu_e$ -disappearance test:

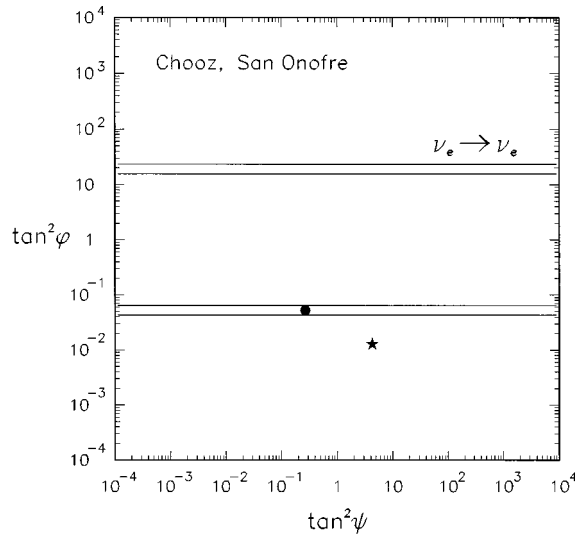


FIG. 4. Allowed bands corresponding to the  $\nu_e \rightarrow \nu_e$  disappearance test at reactors (Chooz, San Onofre). This test appears to solve the twofold ambiguity between the “true” (•) and “false” (\*)  $3\nu$  mixing solution in Figs. 2 and 3.

$$Q_{ee} \equiv 1 - P_{ee}. \quad (14)$$

In the  $3\nu$ -mixing test case [Eq. (4)],  $Q_{ee} = 0.095(1 \pm 0.2)$ . This value is in the sensitivity region of the Chooz [8] and San Onofre [9] experiments.

In Fig. 4 we show the corresponding isosignal stripes. It can be seen how the supplementary reactor  $\nu$  information singles out the “true” mixing case (•) and solves the ICARUS and MINOS ambiguity.

However, at slightly smaller test values of  $\phi$  the reactor experiments become rapidly less sensitive and might not be able to select the “true” solution within the errors.

## VI. SUMMARY

We have studied tests of three-flavor mixing in future long-baseline  $\nu$  oscillation experiments. We have adopted a specific, simple  $3\nu$ -mixing case [Eq. (4)], highlighting the aspects that have a more general validity.

We have considered five observables,  $Q_{\mu e}$ ,  $Q_{\mu\tau}$ ,  $Q_T$ ,  $Q_{f/n}$ , and  $Q_{ee}$ , that assume nonzero values in the presence of oscillations. A large fraction of the  $Q_T$  and  $Q_{f/n}$  oscillation signals (MINOS) is related to  $\mu$  disappearance, and their combination may not be very effective in constraining  $3\nu$ -mixing cases. The flavor-appearance observables  $Q_{\mu\tau}$  (ICARUS) and  $Q_{\mu e}$  (ICARUS, MINOS) allow a better resolution of  $3\nu$  mixing angles, modulo a residual twofold ambiguity. The addition of the reactor observable  $Q_{ee}$  (Chooz, San Onofre) may solve the ambiguity and select a unique  $3\nu$  signal.

## ACKNOWLEDGMENTS

We thank J. H. Cobb, M. Goodman, P. I. Krastev, and D. Petyt for reading the manuscript and for useful information and suggestions. We thank the organizers of the Gran Sasso Long-baseline Workshop (Gran Sasso, Italy), where preliminary results of this work were presented. This work was supported by INFN and by the Institute for Advanced Study.

- 
- [1] MINOS Collaboration proposal, Fermilab Report Nos. NuMI-L-63 and NuMI-L-79 (unpublished).
  - [2] “Subpanel of the High Energy Physics Advisory Panel on Accelerator-based Neutrino Oscillation Experiments,” U.S. Department of Energy Report No. DOE-ER-0662, 1995 (unpublished).
  - [3] KEK-PS and SuperKamiokande Collaboration proposal, University of Tokyo report, 1995 (unpublished).
  - [4] E889 Collaboration proposal, Brookhaven National Laboratory Report No. BNL-52459 (unpublished).
  - [5] ICARUS Collaboration proposal, Laboratori Nazionali del Gran Sasso (LNGS, Italy) Report Nos. LNGS-94-99 (Vols. I and II) and LNGS-95-10 (unpublished).
  - [6] T. Ypsilantis *et al.*, CERN Report No. CERN-LAA-96-02 (unpublished).
  - [7] NOE Collaboration, Letter of intent to the Scientific Committee of Gran Sasso Laboratory (1995), University of Naples report (unpublished).
  - [8] Chooz Collaboration proposal, Collège de France report, 1993 (unpublished).
  - [9] San Onofre Collaboration proposal, California Institute of Technology report, 1994 (unpublished).
  - [10] G. L. Fogli, E. Lisi, and G. Scioscia, Phys. Rev. D **52**, 5334 (1995).
  - [11] G. L. Fogli, E. Lisi, and D. Montanino, Phys. Rev. D **49**, 3626 (1994); Astropart. Phys. **4**, 177 (1995).
  - [12] G. L. Fogli and E. Lisi, Phys. Rev. D **52**, 2775 (1995).